Am J Transl Res 2023;15(2):1007-1016
www.ajtr.org /ISSN:1943-8141/AJTR0143059

Original Article

Aucubin protects against retinal ganglion cell injury in diabetic rats via inhibition of the p38MAPK pathway

Mei Feng, Xia Jiang, Qingsong Zhang, Qifeng Wang, Chunyan She, Zudan Li

Aier Eye Hospital of Wuhan University, Wuhan 430063, Hubei, China

Received March 23, 2022; Accepted December 25, 2022; Epub February 15, 2023; Published February 28, 2023

Abstract: Objective: To explore the role of aucubin in regard to injured retinal ganglion cells (RGCs) in diabetic rats and its mechanism. Methods: A rat model of diabetes mellitus was created by single intraperitoneal injection of 55 mg/kg of streptozotocin. Rats were treated with intraperitoneal injection of 1, 5, and 10 mg/kg aucubin or 5 μg/kg p38MAPK inhibitor SB203580, once a day, for 28 consecutive days. Body weight, blood glucose, morphological changes, count and apoptosis of RGCs, p38MAPK signaling pathway, apoptosis-related proteins, oxidative stress indices, and inflammatory factors were observed and compared among the groups. Results: Aucubin and SB203580 reduced the abnormality of the photoreceptor layer, bipolar cell layer and RGCs. Aucubin significantly reduced body weight, fasting blood glucose, RGC apoptosis rate, p38MAPK protein phosphorylation level, protein expression of Caspase 3 and Bax, vascular endothelial growth factors (interleukin-1β, intercellular adhesion molecule-1 and tumor necrosis factor-α) and malondialdehyde levels, and increased RGC count and protein expression of Bcl-2 and Bcl-2/Bax ($P < 0.05$). Conclusion: Aucubin can protect RGCs in diabetic rats, inhibit RGC apoptosis, and reduce oxidative stress and inflammatory response, and 10 mg/kg aucubin showed optimal efficacy. The mechanism may be related to the inhibition of the p38MAPK signaling pathway.

Keywords: Diabetes mellitus, retinal ganglion cells, aucubin, p38MAPK signaling pathway

Introduction

Diabetic retinopathy (DR) as a common chronic microvascular complication of diabetes mellitus (DM), is caused by increased retinal vascular permeability due to abnormal glucose and lipid metabolism, resulting in intraretinal proliferation and obstruction, stimulating neovascularization and inducing microvascular injury [1, 2]. Epidemiological data showed that in 2015 about 216 million DR patients worldwide were visually impaired, and 36 million were blind, indicating that DR has become a major cause of visual dysfunction and even blindness [3]. The pathogenesis of DR is complex and is regulated by many mechanisms, including oxidative stress, hexosamine pathway, polyol pathway, protein kinase C pathway and advanced glycosylation end products, as well as by blood pressure, glucose, lipids and obesity [4, 5]. It has been found that injury in retinal ganglion cell (RGC) axons form the optic nerve is the main pathological change in the development and progression of DR [6]. Therefore, early prevention and treatment of reduced RGCs or increased apoptosis are key to inhibit disease progression and improve prognosis.

p38MAPK is a stress response pathway that transmits intracellular and extracellular signaling stimuli, and activated p38MAPK entering the nucleus can cause cell cycle arrest, apoptosis and senescence, and induce cellular immune response or inflammatory response [7]. High glucose levels can aggravate the phosphorylation of p38MAPK and activate the p38MAPK signaling pathway [8]. Studies have shown [9] that hyperglycemia is an activator of p38MAPK, and oxidative stress is enhanced under a high glucose environment. Signal stimulation such as oxidative stress can further activate p38MAPK phosphorylation, and p-p38MAPK activates Caspase-3 downstream to initiate the process of apoptosis in peripheral neuronal cells, resulting in RGC cell damage. Aucubin is an iridoid glycoside, with the chemical name of β-D-glucopyranoside, and it is one of the effective components of

Chinese herbal medicines such as Eucommia ulmoides, plantain and rehmannia [10]. Aucubin has a wide range of pharmacological effects, including reducing inflammatory response, endoplasmic reticulum stress response and oxidative stress response, thereby reducing neurological, ocular and cardiovascular damage [11]. Studies have found that aucubin can activate various signaling pathways, e.g., nuclear factor (erythroid-derived 2)-like 2 (Nrf2), AMP-activated protein kinase and nuclear factor-κB, to repair oxidative damage, promote endogenous antioxidant defense and regulate the inflammatory immune response [12]. Meanwhile, some scholars have found that aucubin has a protective effect on acute cerebral hemorrhage, Parkinson's disease and neurons in the diabetic brain [13], but its effect on diabetic RGC damage has not been reported. This study analyzed the effect of aucubin on RGCs in diabetic rats and the involvement of the p38MAPK signaling pathway, aiming to provide new drug options for DR.

Materials and methods

Materials

Sixty male Sprague-Dawley (SD) rats (180-220 g, 6-8 weeks old) were supplied by Shanghai JSI Laboratory Animal Co., Ltd., with animal use approval No. SYXK (Shanghai) 2018-0004. Animals were housed at a temperature of (24 ± 1)°C, relative humidity of 60%, and in 12 h/12 h light/dark cycle. All animals were checked for normal blood glucose by a blood glucose meter (Shanghai Yuyan Scientific Instruments Co., Ltd., China), and no lesions were seen by slit lamp examination. All experimental procedures were in accordance with the relevant requirements in the Regulations of the People's Republic of China on the Administration of Laboratory Animals and approved by the Animal Care and Use Committee of Aier Eye Hospital of Wuhan University.

Methods

Model establishment and grouping: Fifty male SD rats were given intraperitoneal injection of 55 mg/kg of streptozotocin (Beijing Solarbio Science & Technology Co., Ltd., China) (dissolved using pH 4.5, 0.1 mol/L sodium citrate solution) to establish the DM rat model. The criterion for successfully establishment of DM rat model was that the tail vein fasting blood glucose (FBG) level of rats exceeded 16.7 mmol/L after 72 h of induction. A total of 50 rats were modeled and the successful rate was 100%. The 50 DM modeled rats were randomized to the model group (MG), low dose group (LDG), middle dose group (MDG), high dose group (HDG) and SB203580 group, with 10 rats in each group. Among them, all the groups except the MG were given corresponding drug treatments. The LDG, MDG and HDG were injected intraperitoneally with 1, 5 and 10 mg/kg of aucubin (98% purity, Shanghai Yuntai Information Technology Co., Ltd., China), respectively. The SB203580 group was injected intraperitoneally with 5 μg/kg of p38MAPK inhibitor (CalBio-Chem, Inc., USA). The MG was injected intraperitoneally with equal volume of normal saline. Another 10 male SD rats were enrolled as the control group (CG). The rats were injected intraperitoneally with the equal amount of normal saline, 1 time/d, for 28 d. The body weight and FBG level were measured before and 28 d after administration.

Sample preparation: Two hours after the last administration, the rats were generally anesthetized by an intraperitoneal injection of 1 mL/100 g of 0.3% sodium pentobarbital. We opened the thorax to fully expose the heart, cut open the right auricle, and rapidly perfused each animal with about 250 mL of 4% paraformaldehyde into the left ventricle. Then, we disinfected the skin around the bilateral eyeballs, clamped up the bulbar conjunctiva using sterile forceps, and cut open the superior rectus muscle to expose the optic nerve. As the optic nerve was bluntly separated and exposed, the eyeballs were disconnected at 2 mm posterior to the eye. The bilateral eyeballs were removed and placed in pre-chilled 4% paraformaldehyde and normal saline. The eyeballs were cut along the corneal margin. The vitreous and lens were removed, and the retina was separated for later use.

Pathological histology: The fixed posterior segments were taken, dehydrated with ethanol, cleared with xylene, embedded with paraffin, serially sectioned into 3 μm thickness using a paraffin slicer (Leica, Germany). The sections were hydrated with descending concentrations of ethanol (100%, 95%, 90%, 80%, 70%), soaked for 3 min, stained with hematoxylin for 10 min, rinsed with tap water, stained with eosin

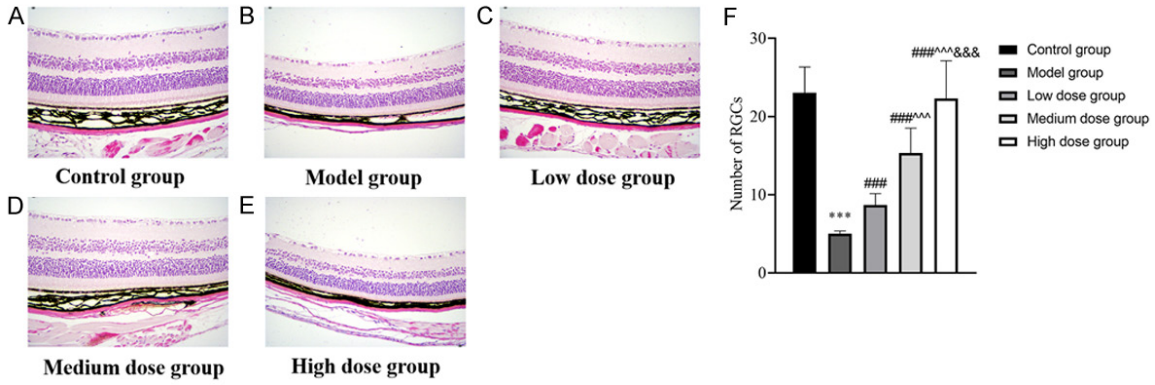

Figure 1. H&E staining of retinal tissue in each group (n = 10). A: In the control group, the nuclei of retinal ganglion cells (RGCs) were clear and neatly arranged in a single layer, and the outer bipolar cells and photoreceptor epithelial cells were tightly and neatly arranged. B: The count of cells in the photoreceptor layer and bipolar cell layer decreased in the model group, and the RGCs were disordered with sparse nuclei. C-E: The abnormalities of photoreceptor layer, bipolar cell layer and RGCs in the low dose group, medium dose group and high dose group were less than those in the model group. F: Number of RGCs. Note: Compared with the control group, $^{***}P < 0.001$; compared with the model group, $^{###}P < 0.001$; compared with the low dose group, $^{\wedge\wedge\wedge}P < 0.001$; compared with the medium dose group, $^{\&\&\&}P < 0.001$.

for 5 min, and rehydrated with descending concentrations of ethanol (70%, 80%, 90%, 95%, 100%) for 3 min. After dehydration, the slides were mounted. The histopathological changes were observed under an optical microscope (Shenzhen Zico Biotechnology Co., Ltd., China), and the RGC count was observed using Image J software.

Flow cytometry: Retinal specimens were taken, and single cell suspensions were prepared. The concentration of cells was adjusted to $\times 10^9$/L and processed according to the instructions of Annexin V/PI kit (Pharmingen, Saratoga, USA). The 100 μL of cell suspension, 5 μL of 7-ADD and 5 μL of FTTC Annexin V were mixed thoroughly and placed at room temperature (20-25°C) for 15 min away from light, followed by adding 400 μL of binding buffer. The apoptosis rate was immediately detected on the machine.

Western blot: The retinal specimens were added to the buffer solution and centrifuged for 15 min (4°C, 12000 rpm). The supernatant was obtained and aliquoted for cryopreservation. The sample was diluted with lysate, collected, loaded, and heated for 5 min, and the proteins were denatured and separated by gel electrophoresis. Next, the proteins were transferred to a PVDF membrane, decolorized at room temperature, shaken and sealed for 2 h. Then, primary (1:500 dilution) and secondary (1:2000 dilution) antibodies were added and incubated for 2 h at room temperature, followed by washing the membrane 3 times with PBS (Beijing Taizejiaye Technology Development Co., Ltd., China), 15 min each time. The primary antibodies, including p38MAPK (No. 9926), p-p38MAPK (No. 9910), TrkB (No. 4603), p-TrkB (No. 4603P), JNK (No. 4668S), p-JNK (No. 9251), ERK (No. 9102), p-ERK (No. 3179), Bax (No. 2772), Caspase-3 (No. 9662), Bcl-2 (No. 2872) and GAPDH (No. 5174), were supplied by CST Biotechnology Co., Ltd., USA. The secondary antibody, horseradish peroxidase-labeled goat anti-rabbit immunoglobulin (Ig) G (No. bs-0295G-HRP), was supplied by Shanghai Jianglai Biotechnology Co., Ltd., China. ECL luminescent solution was used for color development, and Image J software was used for quantitative analysis. GAPDH (1:1000 dilution) was used as an internal reference, and the ratio indicated the relative expression of the target protein.

Immunohistochemistry and enzyme-linked immunosorbent assay: Retinal specimens were homogenized, and immunohistochemistry was applied to determine the serum levels of malondialdehyde (MDA), superoxide dismutase (SOD), and glutathione peroxidase (GSH-PX), with immunohistochemical assay kits supplied by Shanghai Yaji Biotechnology Co., Ltd., China. Enzyme-linked immunosorbent assay (ELISA) was performed to determine the levels of vascular endothelial growth factor (VEGF), interleukin (IL)-1β, intercellular adhesion molecule-1

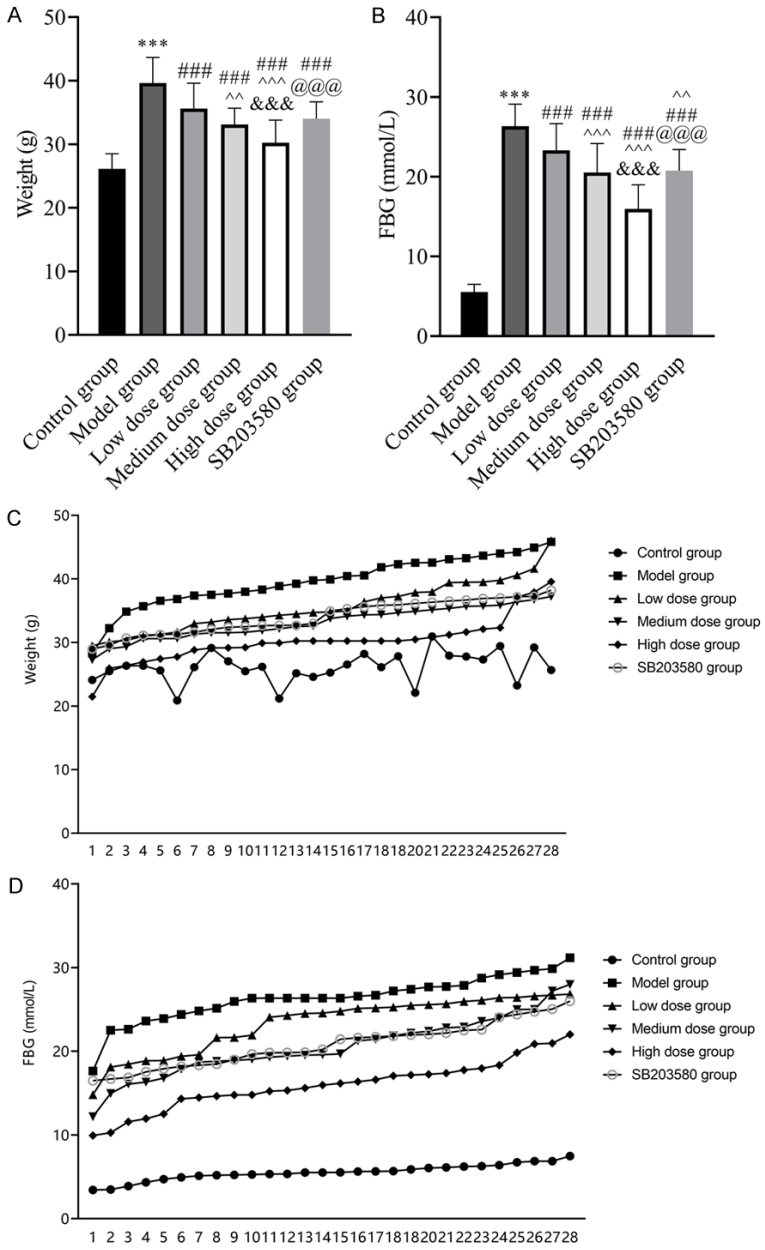

Figure 2. Comparison of body weight and fasting blood glucose (FBG) (n = 10). A: Weight; B: FBG; C: Changes in body weight during 0-28 days; D: Changes in FBG during 0-28 days. Note: Compared with the control group, $^{***}P < 0.001$; compared with the model group, $^{\#\#\#}P < 0.001$; compared with the low dose group, $^{\wedge\wedge}P < 0.01$, $^{\wedge\wedge\wedge}P < 0.001$; compared with the medium dose group, $^{\&\&\&}P < 0.001$; compared with the high dose group, $^{@@@}P < 0.001$.

(ICAM-1) and tumor necrosis factor (TNF)-α, with ELISA kits supplied by Unilever (Shanghai) Life Science Co., Ltd., China.

Statistical analysis

SPSS 24.0 was used for statistical analysis. GraphPad Prism 8 software was used to plot the graphs. The data with normal distribution were described by mean ± standard deviation (mean ± SD), and one-way analysis of variance with post hoc least significant difference-t test was adopted for comparison among multiple groups. $P < 0.05$ was considered statistically significant.

Results

Effect of aucubin on the morphology and count of RGCs

In the CG, the nuclei of RGCs were clear and neatly arranged in a single layer, and the outer bipolar cells and photoreceptor epithelial cells were tightly and neatly arranged. The count of cells in the photoreceptor layer and bipolar cell layer decreased in the MG, and the RGCs were disordered with sparse nuclei. The abnormalities of the photoreceptor layer, bipolar cell layer and RGCs in the LDG, MDG and HDG were less than those in the MG. In addition, the photoreceptor cells in the SB203580 group were arranged in an orderly manner with clear nuclei. The RGC count in the MG was lower than that in the CG and the SB203580 group ($P < 0.05$). The RGC count was the highest in the HDG, followed by MDG and LDG, and the lowest in MG. It is indicated that both aucubin and SB203580 can protect the count and morphology of RGCs in diabetic rats (**Figure 1**).

Effects of aucubin on the body weight and FBG level

The body weight and FBG of the MG were higher than those of the CG before treatment and on the 28th day ($P < 0.05$). The body weight and FBG of the SB203580 group were lower than those of the MG on the 28th day ($P < 0.05$). The

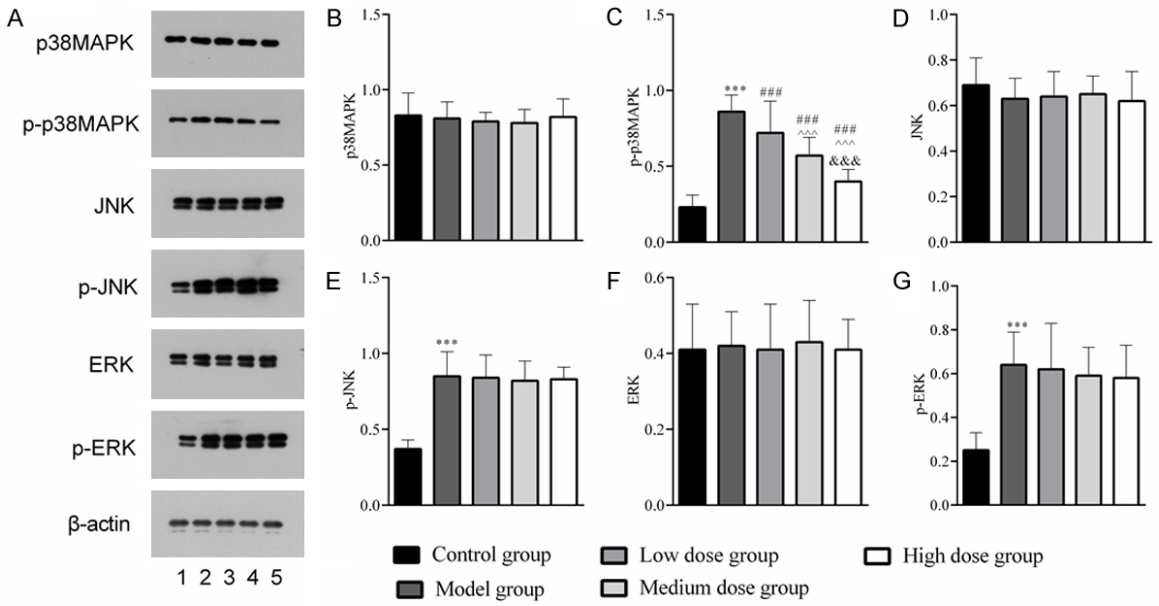

Figure 3. Comparison of relative expression of p38MAPK signaling pathway in the retina tissue (n = 10). A: Western blot images of relative expression (1: control group, 2: model group, 3: low dose group, 4: medium dose group, 5: high dose group); B: p38MAPK; C: p-p38MAPK; D: JNK; E: p-JNK; F: ERK; G: p-ERK. Note: Compared with the control group, $^{***}P < 0.001$; compared with the model group, $^{\#\#\#}P < 0.001$; compared with the low dose group, $^{\wedge\wedge\wedge}P < 0.001$; compared with the medium dose group, $^{\&\&\&}P < 0.001$.

body weight and FBG were the lowest in the HDG, followed by the MDG and LDG, and the highest in the MG ($P < 0.05$) on the 28th d of treatment. It is suggested that both aucubin and SB203580 can reduce body weight and FBG levels in diabetic rats (**Figure 2**).

Effect of aucubin on the retinal p38MAPK signaling pathway

Total protein expression levels of p38MAPK, JNK and ERK exhibited no marked differences among all groups ($P > 0.05$). The MG had higher p38MAPK, JNK and ERK protein phosphorylation levels than the CG ($P < 0.05$). The SB203580 group had lower p38MAPK protein phosphorylation level than the MG ($P < 0.05$). The p38MAPK protein phosphorylation level was the lowest in the HDG, followed by the MDG and LDG, and the highest in the MG ($P < 0.05$). The JNK and ERK protein phosphorylation levels exhibited no marked differences among all groups ($P > 0.05$). It is indicated that both aucubin and SB203580 can reduce the degree of p38MAPK phosphorylation and inhibit the activation of p38MAPK signaling pathway in diabetic rats, and high-dose aucubin has the best efficacy (**Figure 3**).

Effect of aucubin on apoptosis rate of retinal cells

The MG had higher apoptosis rate of retinal cells, higher relative protein expression of Caspase3 and Bax, and lower relative protein expression of Bcl-2 and Bcl-2/Bax than the CG did ($P < 0.05$). The SB203580 group showed lower apoptosis rate of retinal cells, lower relative protein expression of Caspase3 and Bax, and higher relative protein expression of Bcl-2 and Bcl-2/Bax than the MG ($P < 0.05$). The apoptosis rate of retinal cells and relative protein expression of Caspase 3 and Bax were the lowest in the HDG, followed by the MDG and LDG, and the highest in the MG. The relative protein expression of Bcl-2 and Bcl-2/Bax were the highest in the HDG, followed by the MDG and LDG, and the lowest in the MG ($P < 0.05$). It is suggested that both aucubin and SB203580 can inhibit the apoptosis rate of retinal cells in DM rats, and high-dose aucubin has the best efficacy (**Figures 4**, **5**).

Effect of aucubin on VEGF and inflammatory factors of retinal tissue

The MG showed higher levels of VEGF, IL-1β, ICAM-1 and TNF-α in the retinal tissue than the

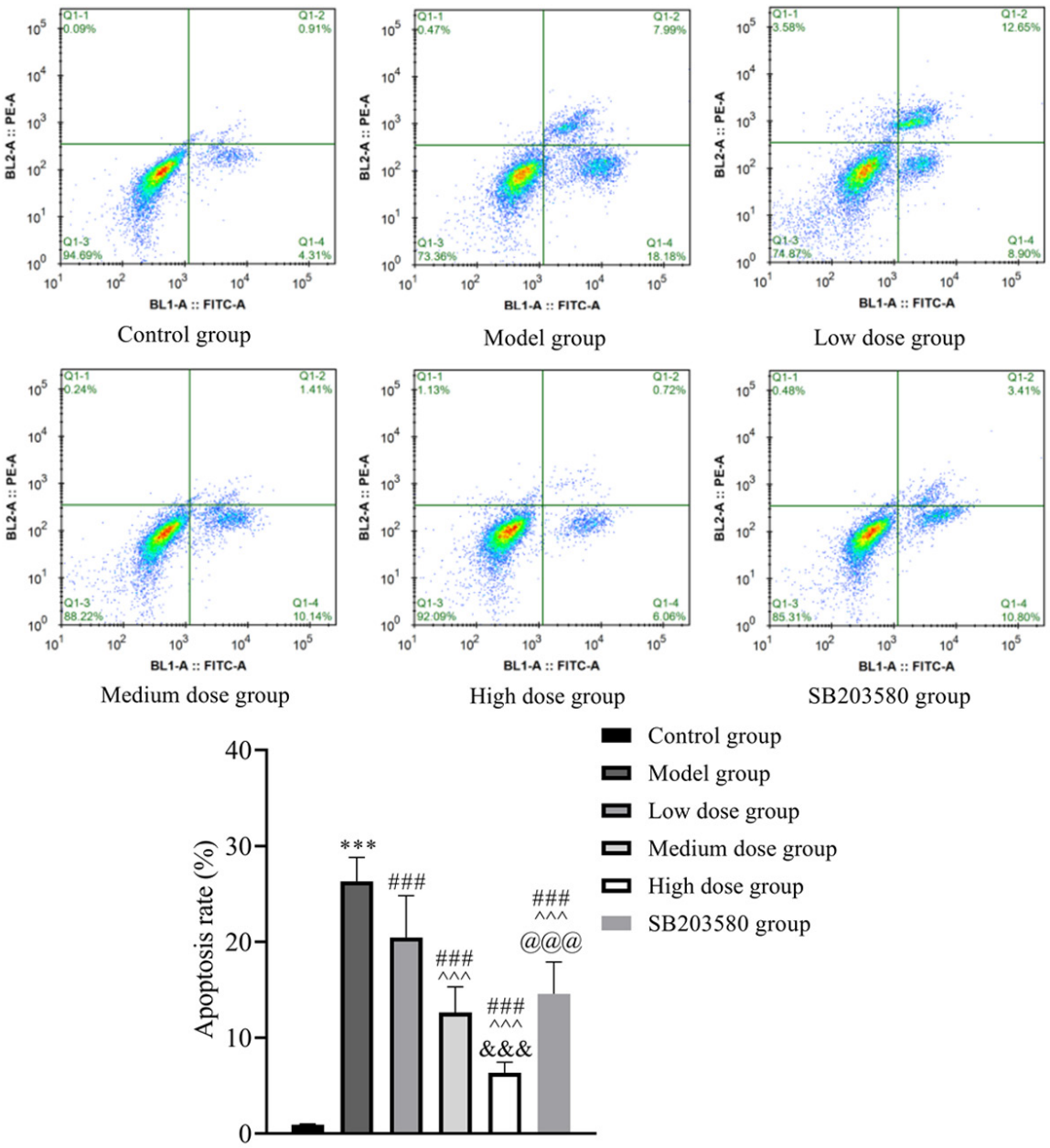

Figure 4. Comparison of apoptosis rate of retinal cells (n = 10). Note: Compared with the control group, $^{***}P < 0.001$; compared with the model group, $^{###}P < 0.001$; compared with the low dose group, $^{\wedge\wedge\wedge}P < 0.001$; compared with the medium dose group, $^{\&\&\&}P < 0.001$; compared with the high dose group, $^{@@@}P < 0.001$.

CG ($P < 0.05$). The SB203580 group showed lower levels of VEGF, IL-1β, ICAM-1 and TNF-α in the retinal tissue than the MG ($P < 0.05$). The levels of VEGF, IL-1β, ICAM-1 and TNF-α levels were the lowest in the HDG, followed by the MDG and LDG, and the highest in the MG ($P < 0.05$). It is indicated that aucubin and SB203580 can inhibit the levels of VEGF and inflammatory factors in the retinal tissue of DM rats and reduce the inflammatory response, and high-dose aucubin exhibits the best effect (**Figure 6**).

Effect of aucubin on the oxidative stress response of retinal tissues

The MD had lower GSH-PX and SOD, and higher MDA in retinal tissue than the CG ($P < 0.05$). The SB203580 group showed higher GSH-PX and SOD levels, and lower MDA in retinal tissue

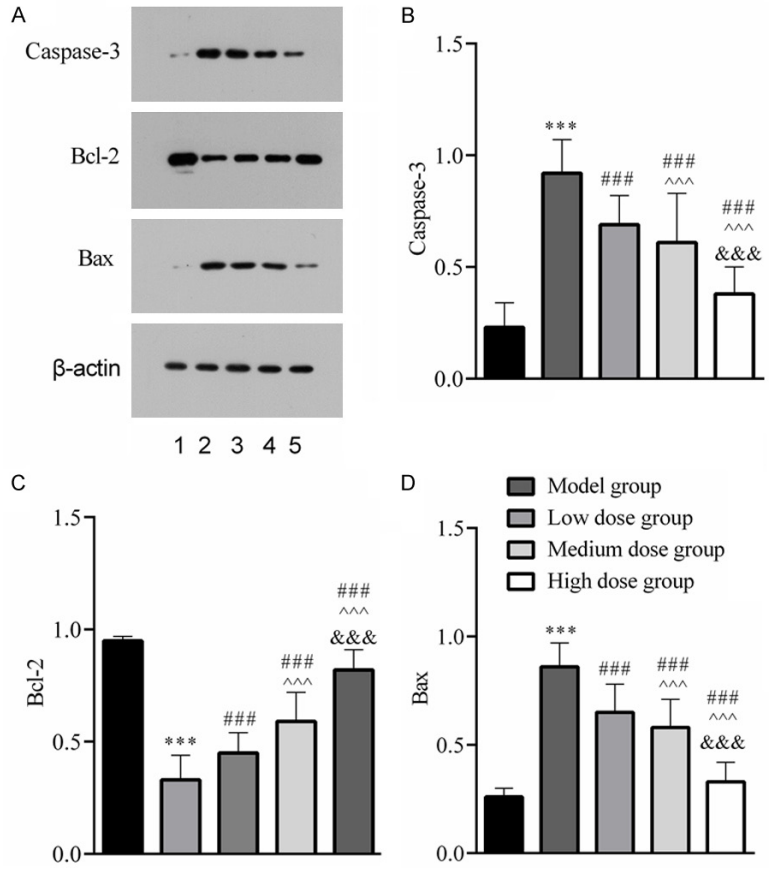

Figure 5. Comparison of relative expression of retinal ganglion cell apoptosis-related proteins (n = 10). A: Western blot images of relative expression (1: control group, 2: model group, 3: low dose group, 4: medium dose group, 5: high dose group); B: Caspase-3; C: Bcl-2; D: Bax. Note: Compared with the control group, $^{***}P < 0.001$; compared with the model group, $^{\#\#\#}P < 0.001$; compared with the low dose group, $^{\wedge\wedge\wedge}P < 0.001$; compared with the medium dose group, $^{\&\&\&}P < 0.001$.

than the MG ($P < 0.05$). The GSH-PX and SOD of retinal tissue were the highest in the HDG, followed by the MDG and LDG, and the lowest in the MG. The MDA levels were lowest in the HDG, followed by the MDG and LDG, and the highest in the MG ($P < 0.05$). It is suggested that both aucubin and SB203580 can reduce the oxidative stress response in the retinal tissue of DM rats (**Figure 7**).

Discussion

As one of the iridoid glycosides, aucubin has pharmacological effects of protecting the nervous system, reducing blood glucose levels, anti-osteoarthritis, and reducing the inflammatory response [13]. Ma et al. [14] found that aucubin promoted endogenous antioxidant defense by inducing sirt1 and sirt3 activity, triggering nuclear translocations of FOXO3a and Nrf2, and upregulating the expression of antioxidant genes such as catalase and heme-oxygenase-1. Besides, aucubin inhibited the nuclear translocation of NF-κB p65, thus inhibiting oxidative stress markers and reducing the inflammatory response. Chen et al. [15] found that aucubin reduced TNF-α, IL-1β and high mobility group protein b1 levels, and weakened the activation and neurotransmission of microglia and astrocyte, thus exerting antiepileptic effects. Xue et al. [16] reported that aucubin effectively regulated blood glucose levels, reduced lipid oxidation production, and improved antioxidant enzyme activity, thereby inhibiting the apoptosis of neuronal cell in hippocampal CA1 region of DM rats. Kim et al. [17] showed that aucubin promoted the proliferation and differentiation of neurons in neural stem cells and contributed to the repair of the peripheral nervous system after nerve injuries. The above studies indicate that aucubin may be a potential neuroprotective agent and a natural drug for the prevention of DM-induced DN. In our study, compared with the CG, the photoreceptor layer, bipolar cell layer and RGCs in the MG were markedly abnormal, and the levels of IL-1β, ICAM-1, TNF-α and MDA were highly expressed in the retinal tissue of the MG, which showed that under the continuous stimulation of high glucose levels *in vivo*, the retinal tissue of DM rats showed obvious inflammatory response and oxidative stress. In contrast, the body weight and FBG of rats decreased after treatment with aucubin, and the expression of inflammatory factors and inducible enzymes were significantly reduced, which confirmed that aucubin can reduce inflammatory damage and oxidative stress.

p38MAPK is widely distributed in the cytoplasm and is a common pathway for many intracellu-

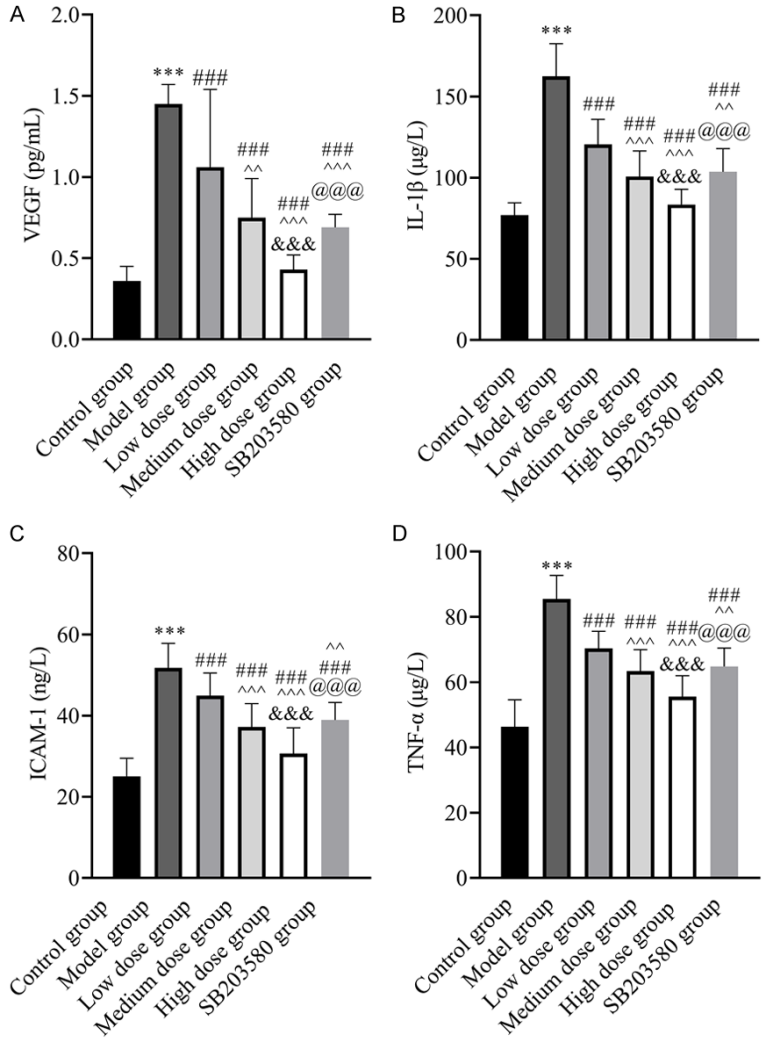

Figure 6. Comparison of vascular endothelial growth factor (VEGF) and inflammatory factors in the retinal tissue (n = 10). A: VEGF; B: Interleukin (IL)-1β; C: Intercellular adhesion molecule-1 (ICAM-1); D: Tumor necrosis factor (TNF)-α. Note: Compared with the control group, $^{***}P < 0.001$; compared with the model group, $^{###}P < 0.001$; compared with the low dose group, $^{\wedge\wedge\wedge}P < 0.001$; compared with the medium dose group, $^{\&\&\&}P < 0.001$; compared with the high dose group, $^{@@@}P < 0.001$.

lar signal transmissions. It can be initiated by oxidative stress signaling and it mediates apoptosis signaling pathways [18-20]. Liu et al. [21] established a DM rat model by intraperitoneal injection of streptozotocin and found that the expression of p-p38MAPK and p-JNK were elevated in the retina of the MG, indicating that changes in the expression of p-p38MAPK and JNK were involved in DM induced retinal lesions. Li et al. [22] reported that the p38MAPK signaling pathway was crucial in DM-induced DR development, and p38MAPK inhibitors reduced early RGC apoptosis and early retinal barrier disorder in DM rats. Ma et al. [23] found that protein expression of p-p38MAPK, caspase-3 and Bax were markedly elevated, while protein expression of Bcl-2 was declined in DR rats, which are similar to our results, further suggesting that the inhibition of the p38MAPK pathway is particularly important to reduce the degree of lesions and apoptosis. In this study, the RGC count was reduced, and the apoptosis rate of RGCs as well as the phosphorylation levels of p38MAPK, JNK and ERK proteins were elevated in the MG, suggesting that the activation of the p38MAPK signaling pathway is closely associated with cell apoptosis. The possible mechanisms of action include: (1) under the stimulation of DM with high glucose level, signals such as oxidative stress can stimulate the activation of the p38MAPK signaling pathway, thus activating the downstream protein (Caspase 3), initiating apoptosis signaling and aggravating apoptosis in peripheral nerve cells, and further damaging RGCs [24, 25]; (2) the activation of the p38MAPK signaling pathway plays a vital role in inducing neuronal apoptosis by NO through promoting the translocation of Bax into the mitochondria [26]. Treatment of SB203580 and aucubin increased the RGC count, and decreased the apoptosis rate of RGCs and the level of p38MAPK protein phosphorylation. It is suggested that the effect of aucubin is similar to SB203580 and can protect RGCs by suppressing the activation of the p38MAPK signaling pathway. Moreover, VEGF can improve vascular permeability, damage the tight junctions of retinal vascular endothelial cells, promote extracellular fluid accumulation and vascular leakage, and thus induce endothelial cell proliferation and neovascularization [27]. Our results

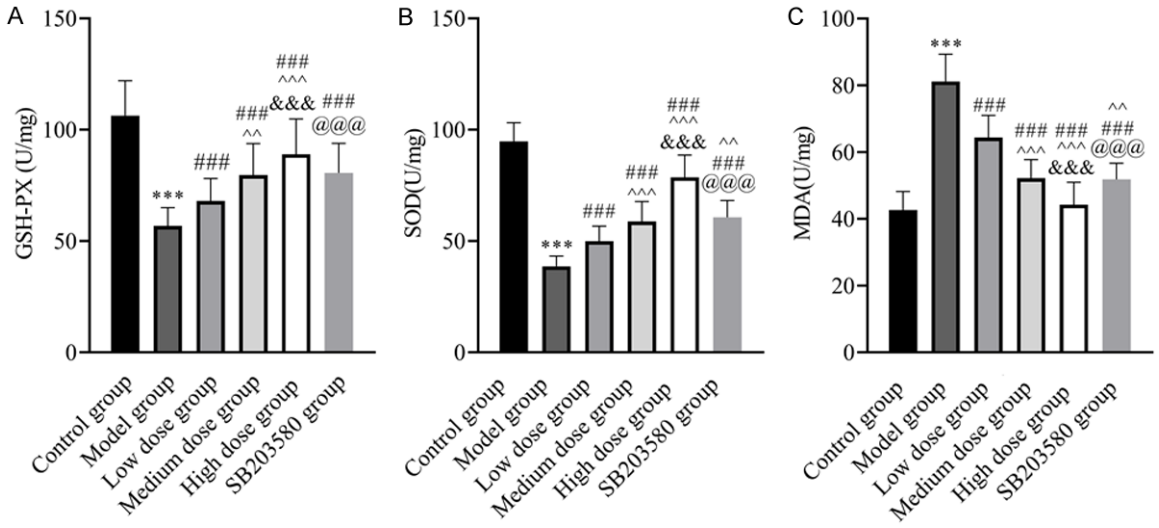

Figure 7. Comparison of the oxidative stress indexes in the retinal tissue (n = 10). A: Glutathione peroxidase (GSH-PX); B: SUperoxide dismutase (SOD); C: Malondialdehyde (MDA). Note: Compared with the control group, $^{***}P < 0.001$; compared with the model group, $^{\#\#\#}P < 0.001$; compared with the low dose group, $^{\wedge\wedge\wedge}P < 0.001$; compared with the medium group, $^{\&\&\&}P < 0.001$; compared with the high dose group, $^{@@@}P < 0.001$.

revealed that aucubin reduced the expression of VEGF in retinal tissue of DM rats, improved retinal microvascular circulation, and ultimately inhibited the progression of DR.

This study provides a new perspective in the pharmacological treatment for patients with DR, and the idea is worthy of further development and research. However, the present study is limited by the small sample size of the experimental animals and the lack of evidence on the specific downstream molecular mechanisms of the relevant pathways, which will be further explored in the next step of our research.

In conclusion, aucubin and SB203580 can protect RGCs in DM modeled rats, inhibit RGC cell apoptosis, reduce oxidative stress and reduce inflammatory response. The dosage of 10 mg/kg of aucubin achieved the best effect, and its mechanism of action may be attributed to the regulation of the p38MAPK signaling pathway.

Acknowledgements

This work was supported by the Wuhan Health and Family Planning Research Foundation (Grant number WX17Q37).

Disclosure of conflict of interest

None.

Address correspondence to: Mei Feng, Aier Eye Hospital of Wuhan University, No. 481, Zhongshan Road, Wuchang District, Wuhan 430063, Hubei, China. Tel: +86-027-68893834; E-mail: fmm5nj@163.com

References

[1] Browning DJ, Stewart MW and Lee C. Diabetic macular edema: evidence-based management. Indian J Ophthalmol 2018; 66: 1736-1750.

[2] Kwan CC and Fawzi AA. Imaging and biomarkers in diabetic macular edema and diabetic retinopathy. Curr Diab Rep 2019; 19: 95.

[3] Schmidt-Erfurth U, Garcia-Arumi J, Bandello F, Berg K, Chakravarthy U, Gerendas BS, Jonas J, Larsen M, Tadayoni R and Loewenstein A. Guidelines for the management of diabetic macular edema by the European Society of Retina Specialists (EURETINA). Ophthalmologica 2017; 237: 185-222.

[4] Romero-Aroca P, Baget-Bernaldiz M, Pareja-Rios A, Lopez-Galvez M, Navarro-Gil R and Verges R. Diabetic macular edema pathophysiology: vasogenic versus inflammatory. J Diabetes Res 2016; 2016: 2156273.

[5] Miller K and Fortun JA. Diabetic macular edema: current understanding, pharmacologic treatment options, and developing therapies. Asia Pac J Ophthalmol (Phila) 2018; 7: 28-35.

[6] Chung YR, Kim YH, Ha SJ, Byeon HE, Cho CH, Kim JH and Lee K. Role of inflammation in classification of diabetic macular edema by

optical coherence tomography. J Diabetes Res 2019; 2019: 8164250.
[7] Feng Y, Fang Z, Liu B and Zheng X. p38MAPK plays a pivotal role in the development of acute respiratory distress syndrome. Clinics (Sao Paulo) 2019; 74: e509.
[8] Singh A, Upadhayay S and Mehan S. Understanding abnormal c-JNK/p38MAPK signaling overactivation involved in the progression of multiple sclerosis: possible therapeutic targets and impact on neurodegenerative diseases. Neurotox Res 2021; 39: 1630-1650.
[9] Chen Y, Zhen HS and Gao J. Protection of diabetic retinal ganglion cells by safflower yellow pigment regulated p38MAPK signaling pathway. Chin Tradit Herb Drugs 2019; 50: 2639-2644.
[10] Ma ZH and Yang ZY. The protective effect of aucubin on Aβ25-35-induced neurite atrophy and neuronal apoptosis. Chin Pharm Bull 2020; 36: 1391-1396.
[11] Zeng X, Guo F and Ouyang D. A review of the pharmacology and toxicology of aucubin. Fitoterapia 2020; 140: 104443.
[12] Wang H, Zhou XM, Wu LY, Liu GJ, Xu WD, Zhang XS, Gao YY, Tao T, Zhou Y, Lu Y, Wang J, Deng CL, Zhuang Z, Hang CH and Li W. Aucubin alleviates oxidative stress and inflammation via Nrf2-mediated signaling activity in experimental traumatic brain injury. J Neuroinflammation 2020; 17: 188.
[13] Yang Z, Wu QQ, Xiao Y, Duan MX, Liu C, Yuan Y, Meng YY, Liao HH and Tang QZ. Aucubin protects against myocardial infarction-induced cardiac remodeling via nNOS/NO-regulated oxidative stress. Oxid Med Cell Longev 2018; 2018: 4327901.
[14] Ma B, Zhu Z, Zhang J, Ren C and Zhang Q. Aucubin alleviates diabetic nephropathy by inhibiting NF-κB activation and inducing SIRT1/SIRT3-FOXO3a signaling pathway in high-fat diet/streptozotocin-induced diabetic mice. J Funct Foods 2020; 64: 103702.
[15] Chen S, Zeng X, Zong W, Wang X, Chen L, Zhou L, Li C, Huang Q, Huang X, Zeng G, Hu K and Ouyang DS. Aucubin alleviates seizures activity in li-pilocarpine-induced epileptic mice: involvement of inhibition of neuroinflammation and regulation of neurotransmission. Neurochem Res 2019; 44: 472-484.
[16] Xue HY, Lu YN, Fang XM, Xu YP, Gao GZ and Jin LJ. Neuroprotective properties of aucubin in diabetic rats and diabetic encephalopathy rats. Mol Biol Rep 2012; 39: 9311-9318.
[17] Kim YM, Sim UC, Shin Y and Kim Kwon Y. Aucubin promotes neurite outgrowth in neural stem cells and axonal regeneration in sciatic nerves. Exp Neurobiol 2014; 23: 238-245.
[18] Herbelet S, Merckx C and De Paepe B. The PKA-p38MAPK-NFAT5-organic osmolytes pathway in duchenne muscular dystrophy: from essential player in osmotic homeostasis, inflammation and skeletal muscle regeneration to therapeutic target. Biomedicines 2021; 9: 350.
[19] Tomida T and Adachi-Akahane S. Roles of p38MAPK signaling in the skeletal muscle formation, regeneration, and pathology. Nihon Yakurigaku Zasshi 2020; 155: 241-247.
[20] Soni S, Anand P and Padwad YS. MAPKAPK2: the master regulator of RNA-binding proteins modulates transcript stability and tumor progression. J Exp Clin Cancer Res 2019; 38: 121.
[21] Liu F, Ma Y and Xu Y. Taxifolin shows anticataractogenesis and attenuates diabetic retinopathy in STZ-diabetic rats via suppression of aldose reductase, oxidative stress, and MAPK signaling pathway. Endocr Metab Immune Disord Drug Targets 2020; 20: 599-608.
[22] Li Y, Lv L, Chen L, Huang X, Zhang J, Li S and Wang X. Protective effect of blocking the signal path of p38 mitogen activated protein kinase on blood retinal barrier and retinal ganglion cells in early diabetic rats. Chin J Ocul Fhundus Dis 2010; 26: 139-142.
[23] Ma Y, Zhao Q, Shao Y, Cao MZ, Zhao M and Wang D. Melatonin inhibits the inflammation and apoptosis in rats with diabetic retinopathy via MAPK pathway. Eur Rev Med Pharmacol Sci 2019; 23: 1-8.
[24] Singh RK and Najmi AK. Novel therapeutic potential of mitogen-activated protein kinase activated protein kinase 2 (MK2) in chronic airway inflammatory disorders. Curr Drug Targets 2019; 20: 367-379.
[25] Ijomone OM, Iroegbu JD, Aschner M and Bornhorst J. Impact of environmental toxicants on p38- and ERK-MAPK signaling pathways in the central nervous system. Neurotoxicology 2021; 86: 166-171.
[26] Stramucci L, Pranteda A and Bossi G. Insights of crosstalk between p53 protein and the MKK3/MKK6/p38 MAPK signaling pathway in cancer. Cancers (Basel) 2018; 10: 131.
[27] Mesquita J, Castro de Sousa JP, Vaz-Pereira S, Neves A, Tavares-Ratado P, M Santos F, A Passarinha L and T Tomaz C. VEGF-B levels in the vitreous of diabetic and non-diabetic patients with ocular diseases and its correlation with structural parameters. Med Sci (Basel) 2017; 5: 17.